

Measurements and Utilization of Consistent Gibbs Energies of Transfer of Single Ions: Towards a Unified Redox Potential Scale for All Solvents

Valentin Radtke,^{*,[a]} Niklas Gebel,^[a] Denis Priester,^[a] Andreas Ermantraut,^[a] Monika Bäuerle,^[a] Daniel Himmel,^[a] Regina Stroh,^[a] Thorsten Koslowski,^[b] Ivo Leito,^[c] and Ingo Krossing^{*,[a]}

Dedicated to Prof. Dr. Jürgen Heinze on the occasion of his 80th birthday

Abstract: Utilizing the “ideal” ionic liquid salt bridge to measure Gibbs energies of transfer of silver ions between the solvents water, acetonitrile, propylene carbonate and dimethylformamide results in a consistent data set with a precision of 0.6 kJ mol^{-1} over 87 measurements in 10 half-cells. This forms the basis for a coherent experimental thermodynamic framework of ion solvation chemistry. In addition, we define the solvent independent $p\epsilon_{\text{abs}}^{\text{H}_2\text{O}}$ - and the $E_{\text{abs}}^{\text{H}_2\text{O}}$ values that account for the electronating potential of any redox system

similar to the $p\text{H}_{\text{abs}}^{\text{H}_2\text{O}}$ value of a medium that accounts for its protonating potential. This $E_{\text{abs}}^{\text{H}_2\text{O}}$ scale is thermodynamically well-defined enabling a straightforward comparison of the redox potentials (reducities) of all media with respect to the aqueous redox potential scale, hence unifying all conventional solvents' redox potential scales. Thus, using the Gibbs energy of transfer of the silver ion published herein, one can convert and unify all hitherto published redox potentials measured, for example, against ferrocene, to the $E_{\text{abs}}^{\text{H}_2\text{O}}$ scale.

Introduction

The (intrinsic) chemical potential μ of a chemical entity is a fundamental thermodynamic state function that reflects its chemical environment (i.e., its bonding conditions, etc.) and allows conclusions to be drawn about how this entity will react to changes in this environment.^[1] In two of the most important reaction classes in chemistry, namely acid-base and redox

reactions, ions, that is, electrically charged entities, are involved. Because of their charge, these entities are affected by electric fields in addition to their chemical environment, and the corresponding state function characterizing these entities is the electrochemical potential $\tilde{\mu}$,^[2] expressed as the sum of μ and φ , the inner or Galvani potential of a phase. φ is the sum of the outer or Volta potential ψ and the surface potential χ . The latter is a property of a pure phase and is caused, for example, by dipole orientations at the phase's surface. The real potential α , defined as the sum of μ and χ , is also of some importance.

In addition, when dealing with electrically charged entities some aspects must be considered that are absent for electrically neutral entities or electrically neutral pairs of entities (e.g., electrolytes), for which μ are observables. First and foremost, it is impossible to prepare and analyze single ion solutions due to the global electroneutrality condition.^[3] For this reason, the definition of $p\text{H}_S$ as $-\lg a(\text{H}^+, S)$ referring to the activity a (which is a μ -based value) of the proton in the solvent S is accepted as notional (S commonly refers to H_2O and is omitted). A measuring protocol is recommended for $S = \text{H}_2\text{O}$ that takes into account the effect of counterions.^[4] With the same reasoning the Nernst equation, containing activities of the redox active species, and thus, the standard hydrogen electrode (SHE_S) as zero point of the redox potential scale, must also be regarded as a notional definition of the electrode potential. Nevertheless, the dependence on counterions does not imply that single ion quantities such as the activity a are meaningless.^[5,6] Experience tells us that the effects of the counterions, for example, in the case of strong acids, are not incisive. In the realm of infinite dilution, these effects vanish leading to the definition of standard states for solutes in solution.^[7]

[a] Dr. V. Radtke, N. Gebel, D. Priester, A. Ermantraut, M. Bäuerle, Dr. D. Himmel, R. Stroh, Prof. I. Krossing
Institut für Anorganische und Analytische Chemie
Freiburger Materialforschungszentrum (FMF)
and Freiburg Center for Interactive Materials and Bioinspired Technologies (FIT)

Albert-Ludwigs-Universität Freiburg
Albertstr. 21, 79104 Freiburg (Germany)
E-mail: valentin.radtke@ac.uni-freiburg.de
krossing@uni-freiburg.de

[b] Prof. T. Koslowski
Institut für Physikalische Chemie
Albert-Ludwigs-Universität Freiburg
Albertstr. 23a, 79104 Freiburg (Germany)

[c] Prof. I. Leito
Institute of Chemistry,
University of Tartu
Ravila 14a Str, 50411 Tartu (Estonia)

Supporting information for this article is available on the WWW under <https://doi.org/10.1002/chem.202200509>

© 2022 The Authors. Chemistry - A European Journal published by Wiley-VCH GmbH. This is an open access article under the terms of the Creative Commons Attribution Non-Commercial NoDerivs License, which permits use and distribution in any medium, provided the original work is properly cited, the use is non-commercial and no modifications or adaptations are made.

Unfortunately, because this definition of standard states is also used as reference for single ions, pH values and redox potentials cannot be compared between different solvents, since they differ in their zero points, and the relative position of the zero points is usually unknown. The reason is that solute-solvent and solvent-solvent interactions are still operative in infinitely dilute solutions, and each solvent molecule interacts differently with a solute molecule and with itself. Therefore, each solvent comes along with an individual reference state, which generally differs from reference states in other solvents.^[8] The remedy is a reference state that is valid for all phases and the measurement with respect to this state would be consequent. However, this endeavor is anything but simple because it is intertwined with the definition of single electrode potentials on the one hand, and with the procedure of measurements on the other.

Trasatti summarized the knowledge of his time, and identified different definitions, based on either $\tilde{\mu}$, α or μ , all bearing the same conceptual validity provided the physically infeasible separation of chemical and electrical contributions is tolerated, and the question is which one can be preferred in terms of applicability.^[9] Preferred by IUPAC is a definition that integrates only principally measurable quantities, which results in the definition including the real potential,^[10] rather than the chemical potential, although the latter is of greater general interest, since it does not depend on “non-chemical” contributions such as surface potentials, but only on internal conditions. If, for example, one would define the pH with α instead of μ , one would agree that the surface potential affects the acidity of a medium, otherwise one would have to tolerate a disparity, in case of the aqueous phase of about 3 pH units. The chemical potential of a single ion, however, has so far been considered unmeasurable. Although experimentally and theoretically determined values for the aqueous phase are reported, they are all controversial and contain so-called extra-thermodynamic assumptions. Hünenberger and Reif give an exhaustive overview, and recommend for the standard Gibbs energy of the proton’s hydration $-1100.0 \text{ kJ mol}^{-1}$ (which is equivalent to $\mu_{\text{H}^+}^{\ominus}(\text{H}_2\text{O})$).^[11,12]

As reference state that is valid for all phases, we use the electron’s intrinsic chemical potential of the ideal electron gas at 10^5 Pa and 298.15 K (i.e., $\mu_{\text{e}^-}^{\ominus}(\text{g}, T) = 0 \text{ kJ mol}^{-1}$).^[13] We defined the unified pe_{abs} value of a medium as in Equation (1). Thus, we effectively relate its potential to the reductivity¹ an electron gas with the pressure $p(\text{e}^-, \text{g}) = 10^{-\text{pe}_{\text{abs}}}$ bar provides to the medium.

$$\text{pe}_{\text{abs}} = -\frac{\mu_{\text{abs}}(\text{e}^-, S)}{RT \ln 10} \quad (1)$$

¹We use the elementary steps electronation and deelectronation in their strict sense, i.e., addition or removal of e^- . Thus, a classically termed ‘oxidant’ is addressed as a ‘deelectronator’ and a ‘reductant’ as an ‘electronator’, if only a single electron transfer as the elementary step takes place. This particle based terminology is related to the acid-base picture, where the terms deprotonation and protonation describe the transfer of a proton between two partners, i.e., deelectronation is the electron-based equivalent to a deprotonation. This terminology has been introduced in ref. 13 and 21.

$$E_{\text{abs}} = \text{pe}_{\text{abs}} \frac{RT}{F} \ln 10 = \text{pe}_{\text{abs}} \cdot 0.05916 \text{ V at } 298.15 \text{ K} \quad (2)$$

E_{abs} as given by Equation (2) essentially corresponds to Trasatti’s μ -based single electrode potential $E_{\text{T}}^{\text{[14]}}$ that can be traced back to Kanevskii.^[15] Analogously, the pH_{abs} value was defined by means of the proton’s intrinsic chemical potential with respect to the ideal proton gas at 10^5 Pa and 298.15 K as reference state (i.e., $\mu_{\text{H}^+}^{\ominus}(\text{g}, T) = 0 \text{ kJ mol}^{-1}$).^[16] Hence, a medium is as protonating as a proton gas with the pressure $p(\text{H}^+, \text{g}) = 10^{-\text{pH}_{\text{abs}}}$ bar. These gaseous reference states, although hypothetical, are well defined and in accordance with IUPAC recommendations.^[7,12,17] Both scales were combined leading to the protoelectric potential map (PPM), allowing the comparison of acidity and reductivity (i.e., reduction power or reduction potential) between all isotropic and homogeneous media.^[13] The situation is illustrated in Figure 1, where the conventional pH_S and SHE_S scales are integrated to the unifying pH_{abs} and pe_{abs} scales constituting the PPM. Included is the $E_{\text{abs}}^{\text{H}_2\text{O}}$ value, which we define in the same manner as the $\text{pH}_{\text{abs}}^{\text{H}_2\text{O}}$ value of a medium,^[18] Equation (3), to align the zero value (not the zero point, that is, the reference state) of the pe_{abs} scale to the $\text{SHE}_{\text{H}_2\text{O}}$ scale. Hence, $\text{pe}_{\text{abs}}^{\ominus}(\text{H}^+/\text{H}_2, \text{H}_2\text{O})$ is the pe_{abs} value of the $\text{SHE}_{\text{H}_2\text{O}}$.

$$E_{\text{abs}}^{\text{H}_2\text{O}} = (\text{pe}_{\text{abs}} - \text{pe}_{\text{abs}}^{\ominus}(\text{H}^+/\text{H}_2, \text{H}_2\text{O})) \frac{RT \ln 10}{F} = \text{pe}_{\text{abs}}^{\text{H}_2\text{O}} \frac{RT \ln 10}{F} \quad (3)$$

In this way, the $E_{\text{abs}}^{\text{H}_2\text{O}}$ scale serves as a thermodynamically well-defined link for the reductivity in all media with respect to the aqueous phase. Yet, this is still the theoretical and conceptual level. The issue of experimental determination of those values is incomparably more difficult.

Direct measurements with respect to the particular gaseous standard states would be the logical step towards the experimental development of unifying scales. However, even the α -based single electrode potential scale suffers from intricate experimental difficulties, and the value obtained for the aqueous phase ($E_{\alpha}(\text{SHE}_{\text{H}_2\text{O}}) = 4.44 \text{ V}$)^[10] has remained without counterparts for other solvents so far. This is also true for the μ -based scales. Moreover, their values are more disputed due to the extra-thermodynamic assumptions made. Therefore, instead of performing such difficult and controversial methods for each phase, it seems much easier to determine differences of Gibbs solvation energies, that is, Gibbs transfer energies. But even in this case, hitherto only methods based on extra-thermodynamic assumptions were reported, although recently an assumption-free method has been proposed, which has not yet been realized in experiment.^[5] In addition, however, for referencing to the gas phase at least one Gibbs solvation energy as an anchor point is needed. Nevertheless, since the relative positions are preserved even if the anchor point shifts, the determination of reliable Gibbs transfer energies is a very worthwhile target. Therefore, we address here the decades-old question of the direct measurability of the elusive Gibbs energy of transfer $\Delta_{\text{T}}G(i, S_1 \rightarrow S_2)$ of a single ion i between the solvents

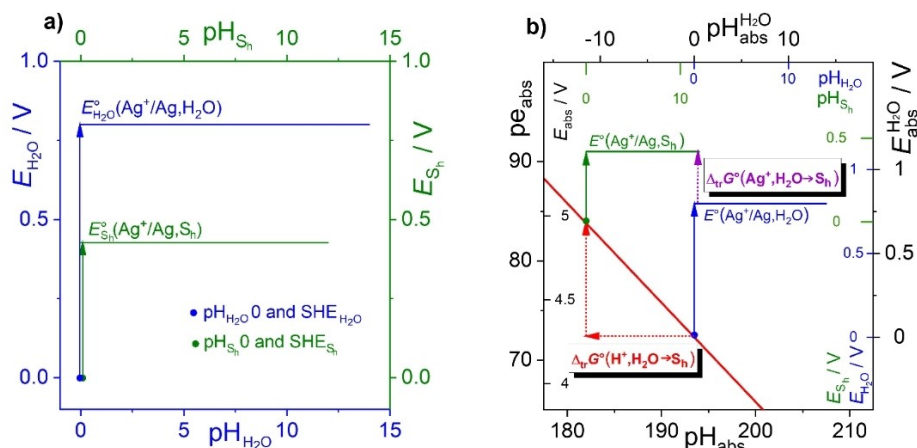


Figure 1. a) The redox system $\text{Ag}^+(\text{soln})/\text{Ag}(\text{s})$ in H_2O and in a hypothetical solvent S_h in the presentation of the conventional pH_5 and SHE_5 scales at $a(\text{Ag}^+, \text{S})=1$. The zero points of these scales cannot be discriminated due to the standard states used. They are defined analogously by the infinitely dilute solution of the proton. Nevertheless, the zero points are inevitably different, as each solvent has individual properties; in other words, the standard states are solvent dependent. Thus, the intersolvent comparison of acidity and redoxity (reduction power) is not possible. The start of an arrow, (the arrow represents an observable) indicates the zero point of the respective scale. The end of the arrow indicates the standard potential value E_s° . In this example, Ag^+ seems to be less de-electronating (oxidizing) in S_h than in H_2O . b) The same systems and the system $\text{H}^+(\text{soln})/\text{H}_2(\text{g})$ (red line) represented in the PPM. The unifying standard states are defined as the ideal electron gas ($pe_{\text{abs}}=0$) and the ideal proton gas ($\text{pH}_{\text{abs}}=0$) at standard conditions. The Gibbs energy of hydration $\Delta_{\text{sol}}G^\circ(\text{H}^+, \text{H}_2\text{O}) = -1104.5 \text{ kJ mol}^{-1}$ [19] is the only anchor [12] used to tie the standard states to the solvent water and thereby to pH_{abs} and pe_{abs} , respectively. The relative position of the redox systems in the different solvents can easily be identified. This is due to the knowledge of Gibbs energies of transfer $\Delta_{\text{tr}}G^\circ(i, \text{H}_2\text{O} \rightarrow \text{S}_h)$ of an ion i from H_2O to S_h , on the one hand, and due to the unifying standard state serving as a zero point that is valid for all solvents on the other. The transfer energies (indicated by dotted arrows) are the key magnitudes for the realization of an experimental PPM. However, these are elusive quantities so far accessible only with the help of extra-thermodynamic assumptions (see below). In this example, it follows that Ag^+ is indeed more de-electronating in S_h than in H_2O . Note that both dotted red arrows are equivalent, indicating the Gibbs energy of transfer of the proton from water to S_h . If one of the elusive transfer quantities were known, the other could be determined in a thermodynamic cycle. The $\text{pH}_{\text{abs}}^{\text{H}_2\text{O}}$ value is equivalent to the pH_{abs} value being aligned to the zero value of the $\text{pH}_{\text{H}_2\text{O}}$ scale, [18] $E_{\text{abs}}^{\text{H}_2\text{O}}$ is defined by Equation (3).

S_1 and S_2 . We use as main anchor the Gibbs energy of the proton's hydration experimentally assessed by Tissandier et al. that is $\Delta_{\text{sol}}G^\circ(\text{H}^+, \text{H}_2\text{O}) = -1104.5 \text{ kJ mol}^{-1}$ (EC–B convention). This results in $E_{\mu}(\text{SHE}_{\text{H}_2\text{O}}) = E_{\text{abs}}(\text{SHE}_{\text{H}_2\text{O}}) = 4.28 \text{ V}$. [12,19] However, the preparation of electrically charged droplets with biased metal needles is now feasible and new techniques using plasma as gaseous electrodes might lead to new experimental evidence in future. [20]

Methods

The activity a of the species participating in a reaction is connected to the Gibbs energy of this reaction $\Delta_r G$ by the law of mass action (and therefore to the chemical potentials μ of these species). If a reaction is divisible in an electronation [21] (reduction) and de-electronation (oxidation) partial reaction, $\Delta_r G$ is connected to the electric potential difference E_{cell} of an appropriate electrochemical cell by Equation (4).

$$\Delta_r G = -nF E_{\text{cell}} \quad (4)$$

n is the electron number of the cell reaction and F is the Faraday constant. The transfer of a silver ion $\text{Ag}^+(\text{soln}, \text{S})$ from one solvent S_1 to another S_2 can be described by Equation (5), with Equations (5a) and (5b) being the electronation and de-electronation partial reactions.



Similar equations can be derived for any ionic species i . Thus in principle, simply the measurement of the electrical potential difference E_i of the electrochemical cell I is suited to determine the Gibbs energy of transfer $\Delta_{\text{tr}}G(\text{Ag}^+, \text{S}_1 \rightarrow \text{S}_2)$ of the silver ion.



AgZ is a silver salt with the counterion Z^- , whose influence on E_i is amongst others the subject of this article. $\text{Ag}(\text{s})$ is solid silver and is therefore an indicator electrode, which under our conditions is selective to silver ions. A single vertical bar represents a phase boundary. The double dashed vertical bar represents a liquid-liquid junction at which the generally occurring potential drop, the liquid junction potential (LJP), is assumed to be nonexistent. This assumption, however, is not justified across typical junctions. [22] Consequently, a single dashed vertical bar representing a liquid junction along with the LJP would be the correct representation of cell I, and the cell potential then reads as in Equation (6).

set of data for single ion transfer is obtained, to our knowledge for the first time. In this way we have created an “ideal” SB as envisaged by Bates:

“The ideal salt bridge would always generate the same diffusion potential, or, better still, no difference of potential, across the liquid junction, Bridge | Soln. X no matter what the composition or pH of solution X might be.”^[33]

The knowledge of x_{ii} is a prerequisite for the determination of $\Delta_{tr}G(i, S_1 \rightarrow S_2)$ by means of cell II. If x_{ii} were zero, cell II would directly give $\Delta_{tr}G(i, S_1 \rightarrow S_2)$. If x_{ii} were non-zero but constant, the obtained Gibbs transfer energies would be known less accurately. However, a consistent data set would be available, because each S_1/S_2 pair gives rise to an individual, but constant x_{ii} . Parker et al. used electrochemical cells similar to cell II, but with conventional SBs, that is, electrolytes dissolved in solvents, to establish the n-LJP assumption.^[34] These cells contain solvent-solvent interactions, thus part C of the LJP. For one S_1/S_2 pair, x_{ii} might be constant, but a series of measurements are very unlikely to generate a consistent data set, because different solvent-solvent interactions occur for each pair S_i/S_j . It is therefore crucial, whether or not part C is operative when using the “ideal” ILSB, as with an IL in the SB, the *direct* contact between each pair S_i/S_j is avoided completely.

With an intricate method, Izutsu determined that part C is certainly not negligible in most solvent pairs. In particular, at the $H_2O|DMF$ junction (DMF = dimethylformamide) he evaluated the LJP part C as more than 100 mV.^[29] Cox et al. also found significant changes of cell potentials, ascribable to individual LJPs, of more than 100 mV in case of using formamide, water or methanol as solvent in one half-cell instead of aprotic solvents.^[35] They could correlate these contributions with the mutual heats of solvation of the solvents. Here we show, particularly by the use of water and DMF as solvents in one half-cell, that in an arrangement as in cell II, obviously no such solvent-solvent interactions occur between S_1 and S_2 , as there is no boundary between these solvents, thus part C is zero. We further show that the LJP values of all the individual $S|IL$ junctions are constant with a standard deviation σ . This allows to evaluate consistent Gibbs energies of transfer between two solvents S_1 and S_2 . The consistency standard deviation σ is demonstrated by a statistical analysis.

Results

To compute the consistency σ , we assembled a network of half-cells. From these, cell II was built in 87 different combinations with the solvents S_1 and S_2 being water (H_2O), acetonitrile (AN), propylene carbonate (PC) and DMF. The latter were chosen as solvents, which dissolve silver salts AgZ readily and thus are expected to give stable potentials. In addition, part C of the LJP was reported to be maximal for the water-DMF junction.^[29] It was, therefore, of interest to find out, if this contribution C was relevant in our setup. The concentrations of the redox active salt AgZ used were set at 0.1, 1.0 and 10.0 mmol L^{-1} and thus we expected the behavior of the dissolved ions to be almost ideal. As a control, we always implemented the MSA model^[36]

to approximate the activity coefficients of the half-cell electrolytes, and we found only small deviations (max. 2 mV) for the MSA corrected $\Delta_{tr}G^{\circ}(Ag^+, S_1 \rightarrow S_2)$ values (see p. 31f in the Supporting Information).

Choice of Z^- anions for AgZ

Six different Z^- anions were used as counterion for the silver cation (Figure 2). They span the range from rather small and stronger coordinating $[NO_3]^-$, $[BF_4]^-$ to the medium sized $[SbF_6]^-$ and triflate $[OTf]^-$ ($Tf = SO_2CF_3$), the larger triflimide $[NTf_2]^-$ and the huge, almost ideally non-interacting $[PF_6]^-$ ($= [Al\{OC(CF_3)_3\}_4]^-$). The use of different counterions revealed only a minor influence on the cell potential. We deduce that the LJP is mainly determined by the ions of the IL. In any case, if systematic dependencies on, for example, the counterions' size or coordination capability would exist, they increase the absolute magnitude of the consistency σ of the assembled network of half-cells and this would eventually indicate the inapplicability of the approach for a large σ value.

Network of half-cells

Hitherto, only the measurements between H_2O and AN in cell II were published.^[32] Figure 3 shows the entire assembled network (all primary data are included in the Supporting Information, p. 31ff). Mathematically, the network represents an overdetermined system, that is, a system of equations with more equations than unknowns. The approximate solution can be found by the method of least squares. We use an established procedure, the result of which gives an optimized value for each unknown with an individual residue for each equation and an overall uncertainty expressed as σ .^[38] The consistency standard deviation s , successfully used to build consistent pK_a scales with a similar approach,^[39] is essentially equivalent to σ (see p. 29f in the Supporting Information). σ represents an

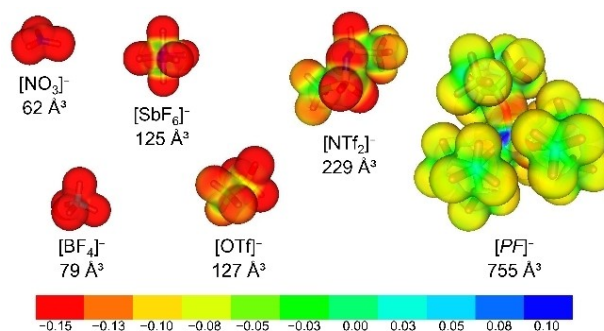


Figure 2. Volumes and electrostatic potentials (plotted on an area of constant electron density of $0.01 e \text{ \AA}^{-3}$) of the Z^- anions used in this work as counterions for the Ag^+ ion. The data were obtained from DFT calculations (RI-BP86/def-TZVP). The ionic volumes were obtained by optimizations with COSMO and scaled by using the equation $V_- = 1.031 V_{-,calc} + 4 \text{ \AA}^3$ (for more details see ref. [37]).

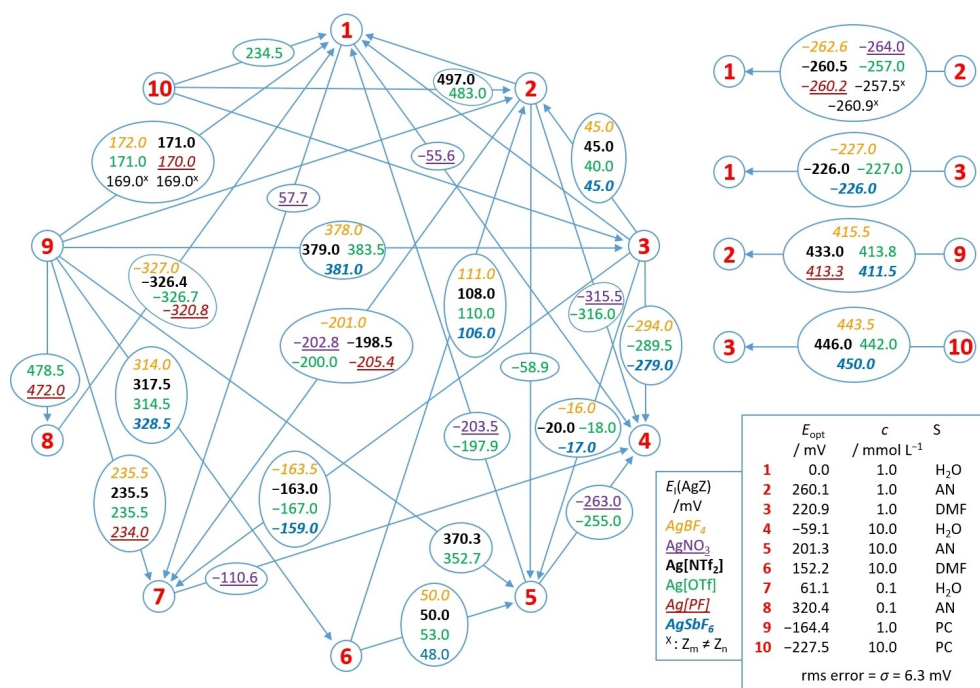


Figure 3. Sketch of the network of the half-cells, indicated by red digits 1...10, with the solvents $S = \text{H}_2\text{O}$, AN, PC and DMF at different AgZ-concentrations (c) in mmol L^{-1} and with different Z^- anions (indicated by colors; Tf = SO_2CF_3 , [PF] = $[\text{Al}(\text{OC}(\text{CF}_3)_3)_4]$). Overall 87 measurements over 10 half-cells were performed. Each arrow between two points of the network symbolizes one distinct implementation of cell II. The starting point of the arrows is the right half-cell and the endpoint the left half-cell. The numbers in the circles superimposed on the arrows are the measured potential differences of cell II E_{ij} in mV with the respective salts AgZ (encoded by colors). Some values are averages. E_{opt} is the optimized potential value with respect to half-cell 1 as the right half-cell obtained by the network analysis (see text).

estimate of the above-mentioned uncertainty of the constancy of x_{lib} , and hence of the constancy of the individual LJPs.

The results of our network analysis and additional literature data are summarized in Table 1. $\Delta_{\text{r}}G^\circ(\text{Ag}^+, \text{S}_1 \rightarrow \text{S}_2)$ values were obtained from the optimized half-cell values 1, 2, 3 and 9 according to Figure 3 with both half cells having a concentration of 1 mmol L^{-1} . The quoted values obtained with different extra-thermodynamic assumptions (TATB, n-LJP and Fc) are discussed and compared to our results in a separate section below. The σ value for the entire network of 87 measurements over 10 half-cells is essentially the rms and was found to be 6.3 mV.

Interference with IL-constituting ions

In the course of this work we observed two cases, where the IL-constituting ions interfere with components of the analytes. These cases present limitations of the method and are inappropriate to be included with the network and the accompanying statistical analysis. They are rationalized in the following:

Low solubility of $[\text{N}_{2225}][\text{NTf}_2]$ in S: We observed with half-cell 4 ($c(\text{AgZ}) = 10 \text{ mmol L}^{-1}$; $S = \text{H}_2\text{O}$) – only if assembled with $\text{Ag}[\text{NTf}_2]$ – deviations in the order of 20–40 mV to all the other salts. The reason is the rather low solubility of $[\text{N}_{2225}][\text{NTf}_2]$ in water, which is only 1.7 mmol L^{-1} (as determined by NMR

Table 1. Optimized values $\Delta_{\text{r}}G^\circ(\text{Ag}^+, \text{S}_1 \rightarrow \text{S}_2)$ as obtained from the network analysis. All energies [kJ mol^{-1} (mol L^{-1} scale)]. The range of individually measured values is given where available. Columns 5, 7 and 9 refer to recommended values obtained with extra-thermodynamic assumptions.^[a]

S_1	S_2	This work Opt.	Range	TATB ^[40] Rec.	Range	n-LJP ^[34] Rec.	Calc. ^[b,c]	Fc ^[40–42] Rec.	Range
AN	H ₂ O	25.1	(24.9–25.5)	23.2	(19.2–31.4)	17.1	17.7 ^[b,c]	37.1	(31.4–39.4)
H ₂ O	PC	15.9	(16.3–16.6)	18.8	(-11.7–22.1)	22.3 ^[a,c]	21.2 ^[b,c]	8.6	–
AN	PC	41.0	(39.7–41.8)	42.0 ^[c]	–	39.4	38.9 ^[b,c]	45.7 ^[c]	–
DMF	H ₂ O	21.3	(21.8–21.9)	20.8	(13.1–41.8)	13.1 ^[a,c]	11.9 ^[b,c]	31.1	(27.4–31.1)
AN	DMF	3.8	(3.9–4.3)	2.4 ^[c]	–	4.0	5.8 ^[b,c]	6.0 ^[c]	–
DMF	PC	37.2	(36.5–37.0)	39.6 ^[c]	–	35.4 ^[a,c]	33.1 ^[b,c]	39.7 ^[c]	–

[a] TATB: $\Delta_{\text{r}}G^\circ(\text{TA}^+) = \Delta_{\text{r}}G^\circ(\text{TB}^-)$ for all S; n-LJP: neglectation of LJPs; Fc: $\Delta_{\text{r}}G^\circ(\text{Fc}) = \Delta_{\text{r}}G^\circ(\text{Fc}^+)$ for all S. These are discussed below. [a] Reference solvent AN; [b] reference solvent methanol; [c] calculated from the given column values (in case of [b] with additional values from Table V in ref. [34]), that is, not directly measurable (TATB and Fc methods) or measured (n-LJP method).

analysis in D₂O). According to the law of mass action the maximum allowed [N₂₂₂₅]⁺-concentration in this particular half-cell 4 is as low as about 0.3 mmol L⁻¹. Thus, the partition of the IL ions, concomitant with the associated LJP value, at this particular 4|IL boundary is different from the other H₂O|IL boundaries in the network. This is generally expected, if solubility product restrictions play a role. Specifically, if one of the ILSB ions and the counterion of the electroactive ion (here: Ag⁺) are identical (here: [NTf₂]⁻) and the IL has a limiting ion solubility lower than the concentration of the analyte (here: 0.3 vs. 10 mmol L⁻¹).

Solubility of [N₂₂₂₅][Z] in S: In half-cell 4, assembled with Ag[PF], the measurements also deviate by about 25 mV. Yet, [N₂₂₂₅][PF] is virtually insoluble in H₂O. Thus, upon diffusion of the IL cation into the half-cell, [N₂₂₂₅]⁺ is withdrawn by precipitation of [N₂₂₂₅][PF] changing its flux and the steady state at the phase boundary, and hence the LJP value. Again, this is generally expected, if solubility product restrictions play a role and specifically here, if the ILSB cation and the counterion (here: [PF]⁻) of the electroactive cation (here: Ag⁺) form a salt insoluble in the solvent of the analyte (here: water).

We also have indications for a third case, where the solubility of Ag[NTf₂] is too low in one of the half-cell solvents. Even if the Ag[PF] salt is well soluble, Ag[NTf₂] is in low polarity solvents such as oDFB (1,2-difluorobenzene) virtually insoluble, and in a metathesis reaction with [N₂₂₂₅][NTf₂] from the ILSB, continuously soluble [N₂₂₂₅][PF] and the insoluble solid Ag[NTf₂] is formed. Thus, through formation of the insoluble salt, the electroactive ion Ag⁺ in S is constantly removed from solution and thus the potentials are continuously shifting during the measurements.

All three cases present – rather special – limitations to the described “ideal” ILSB set up. But currently, we see a huge range of solvents and salts that can be investigated with this method. We point out that this method fails, if it is used to determine Gibbs energies of transfer from molecular solvents into ionic liquids, and we refer to the work of Matsubara et al. in this regard, who extended the TATB assumption for this particular purpose.^[43]

Discussion

First, we turn to the consistency of the assembled network before comparing the results from Table 1 to the Gibbs transfer energies assessed with extra-thermodynamic assumptions. Then we use the optimized values in a unified, solvent independent redox scale.

Consistency of the assembled network

One of the main findings of this work is that the $x_{ii} = E_{j,1} + E_{j,2}$ are consistently constant within 6 mV or 0.6 kJ mol⁻¹. From this, one can deduce some important insights:

α : The LJP at each S|IL junction, although unknown in magnitude, is constant within the rms of 6 mV.

β : In a very good approximation, the LJP at all S|IL junctions depends exclusively on the IL ions. The LJPs are remarkably insensitive against changes of the ionic strength of the electrolyte solutions (due to migration of IL ions into the half-cells) and against the flow of solvent into the ILSB. We continue to investigate the reason for this behavior.

γ : S₁-S₂ interactions are absent. In this context, we stress that the inclusion of DMF into the network would otherwise give completely different results, since direct H₂O|DMF junctions were described by extraordinarily high contributions of H₂O-DMF interactions and the LJP at their boundary to be > 100 mV.^[29] In particular, σ would be much higher.

δ : The experimental determination of x_{ii} becomes possible, at least in principle.

We return to Equation (7), and use the following assumptions and simplifications:

i. The change of t and μ is linear with the solution composition through the phase boundary.

ii. The charge in cell II is exclusively balanced by the IL ions, since the molar concentration of the IL ions in the IL itself is 2.9 mol L⁻¹ – exceeding by far the concentrations of the redox active electrolyte in the investigated solutions.

iii. The diffusion of solvent molecules of the solvent S_i into the ILSB does not contribute to the LJP, since experiments with deliberately added S_i into the ILSB are without effect (see also the Supporting Information of ref. [32]).

Both, ii and iii comply with above point β . Thus, the index of summation in Equation (7) applied on the liquid junctions of cell II reduces to $i = [N_{2225}]^+, [NTf_2]^-$ ($i \neq Ag^+, Z^-, S_1, S_2$). Then Equation (7) results in an equation [Eq. (S6)] complying with Izutsu's Part B-equation^[29] and with Kakiuchi's result for H₂O|IL boundaries.^[44] It can be brought in accord with Equation (6) from Cox et al.^[35] if

iv. the transference numbers of the IL ions are equal throughout the whole cell II. This is reasonable as evidenced by DOSY NMR spectroscopy measurements of the diffusion coefficients of the IL ions in the particular solvents (see p. 26 in the Supporting Information).

With this simplification one can go further and state, if the Gibbs transfer energies of cation and anion of the salt bridge electrolyte are equal:

v. x_{ii} of cell II is negligible.

x_{ii} can be determined by experimental means using suitable ionic systems and Gibbs transfer energies of the corresponding electrolytes. This follows from the fact that the LJPs in cell II are consistently constant. In this way, the assumptions iv and v can be tested. From our perspective, this is a milestone towards the

assumption-free Gibbs transfer energy determination of single ions.

Computation of an expectation value for x_{ii}

To support our observation of a constant or even vanishing x_{ii} , we evaluated x_{ii} by means of quantum chemical methods, since the full experimental determination is sophisticated and exceeds the scope of this work. Hence, the above simplifications i to iv allow to provide Equation (9) for both, the determination as well as calculation of x_{ii} (its derivation is given in the Supporting Information).

$$x_{ii} \cdot F = \frac{1}{2} \Delta_{tr} G^\circ(N_{2225}^+, S_1 \rightarrow S_2) - \frac{1}{2} \Delta_{tr} G^\circ(NTf_2^-, S_1 \rightarrow S_2) \quad (9)$$

Yet, quantum chemical computations of the Gibbs solvation energies of monatomic ions such as Ag^+ or H^+ are tedious and the results are not very reliable, and at least the first solvation shell must be explicitly taken into account.^[45] The electric charge is focused on a small volume, which gives rise to strong ion-dipole interactions. In addition, specific interactions can lead to coordination compounds; consider, for example, the affinity between silver and oxygen or nitrogen donor atoms. For the computation in such cases, parameters must be found to account for accordingly. Delocalized polyatomic ions, with (almost) no “prominent” sites, for example, when atoms of high electronegativity are screened by adequate numbers of other atoms, are in our view less demanding on the solvation model used. The structure of the considered ions is therefore crucial: An even and broad charge distribution in combination with a weak coordination ability allows the use of electrostatic dielectric continuum models like CPCM^[46] without extensive use of empiric parameters that describe specific interactions with the solvent molecules. Considering that our electrolyte ions $[N_{2225}]^+$ and $[NTf_2]^-$ almost ideally qualify for this purpose, they appear predestined for quantum chemical computations. Hence, computations with ORCA 5.0.1^[47] at the rather sophisticated DLPNO^[48]-CCSD(T)/def2-QZVPP^[49] level of theory were performed (see the Supporting Information). DLPNO-CCSD(T) calculations with a large basis set such as def2-QZVPP are considered as the gold standard of computational chemistry. Solvation was implicitly considered at the DLPNO-CCSD(T) level by specifying the CPCM^[46] solvation model, a new implementation only introduced in the last ORCA revision^[47] (Table 2).

Within the limitations of the method, the calculated transfer energies of the two independent ions from S_1 to S_2 in Table 2 are the same within less than $\pm 0.2 \text{ kJ mol}^{-1}$. Thus, the calculated x_{ii} is smaller than 1 mV. It would be audacious to claim that the computational results prove that the accuracy (trueness) of our data is $< 1 \text{ mV}$ for any of the solvent combinations considered. On the other hand, a quite conservative interpretation of these results is that this possibility cannot be completely excluded. Due to the ions' structure, electrostatic effects are expected to dominate, while other non-electrostatic effects are almost unimportant. Therefore, we interpret the

Table 2. Values of $\Delta_{tr} G^\circ$ of the IL ions $[N_{2225}]^+$ and $[NTf_2]^-$ for the transfer from $S_1 \rightarrow S_2$ as obtained from calculations at the DLPNO-CCSD(T)/def2-QZVPP level of theory including the CPCM solvation method. x_{ii} was calculated with Equation (9). Transfer energies in kJ mol^{-1} (mol L^{-1} scale).^[a]

S_1	S_2	$\Delta_{tr} G^\circ / \text{kJ mol}^{-1}$		x_{ii} / mV
		$[N_{2225}]^+$	$[NTf_2]^-$	
AN	H ₂ O	-3.28	-3.10	-0.90
H ₂ O	PC	0.58	0.54	0.24
AN	PC	-2.69	-2.57	-0.66
DMF	H ₂ O	-3.05	-2.87	-0.93
AN	DMF	-0.23	-0.24	0.03
DMF	PC	-2.46	-2.33	-0.69

[a] The relative permittivities of the solvents for the CPCM method were $\epsilon_r = 35.688$ (AN), 78.355 (H₂O), 64.92 (PC) and 37.219 (DMF).

results to reasonably reflect reality, thus supporting assumption v.

Magnitude of the consistency σ and quality of the transfer energies

Equation (8) completely describes the potential difference of cell II, including all interactions occurring in the cell. Thus, any variation of a parameter results in a changed cell potential. And the effects of these changes are statistically represented by the σ value. It does not matter whether the causes of these effects are known in detail. When σ is small, that is, no large effects are observable, simplifications can be made (see points ii and iii above). In this section we discuss how the magnitude of the σ value might originate, but again, since σ is small, so are the effects discussed. Accordingly, the impact of partition equilibria (of the silver salt) is not completely excluded and other effects – which compensate the effects of such equilibria – could be present. The use of different counterions, however, indicates that these effects are small, otherwise σ would be larger. This also is true for S_1 – S_2 interactions, which we claimed above as being absent. Although it is hard to imagine indirect S_1 – S_2 interactions that are operative across the entire salt bridge one could argue with that. However, already our experimental uncertainty, which according to a conservative evaluation amounts to 7–8 mV (see the Supporting Information), may completely explain the σ value. In addition, the implementation of the MSA model to approximate the activity coefficients of the half-cell electrolytes^[32] leads to small deviations (max. 2 mV) for the $\Delta_{tr} G^\circ(Ag^+, S_1 \rightarrow S_2)$ values. The σ values are essentially independent of any MSA correction; a comparison is given in the Supporting Information (p. 31f). Finally, all effects not considered (known or unknown) contribute to the observed standard deviation. Similarly, all deviations from ideality (known or unknown) contribute to an experimentally determined activity coefficient.

Two necessary, but on their own insufficient criteria can be offered to assess the quality of the ionic Gibbs transfer energy values. First, the values obtained for cations and anions must display the (in principle) measurable transfer energy of electrolytes resulting from their combinations. Second, the values for a

specific ion have to be consistent, that is, the sums of the individual transfer energies between the individual solvents have to nullify. The TATB and Fc methods cannot provide the consistency criterion for a specific ion. With reference to our model system with Ag^+ as electroactive ion, this is evident, because practically only one value for the solubility of a salt of Ag^+ (i.e., AgTB) in each solvent is available due to reliability of solubility measurement, and only one value of $E^\circ(\text{Ag}^+/\text{Ag})$ versus $E^\circ(\text{Fc}^+/\text{Fc})$ for each solvent is available. Conversely, electrochemical cells can be built up with different half-cells. Thus, any solvent can be measured more than once and a network analysis becomes possible.

Comparison to the n-LJP assumption

A discussion of the principal differences between the n-LJP assumption and our method is given in the Supporting Information of ref. [30]. The ratio m/n between measured values m and unknowns n , that is, the number of half-cells, of a network is a criterion for the reliability of the results. We applied the network analysis on the values obtained with the negligible liquid junction potential assumption (n-LJP) of Alexander et al.^[34] It gives a modest $m/n = 29/15 = 1.9$ with the consistency standard deviation σ of 1.0 kJ mol^{-1} . Unfortunately, the network topology of Alexander et al.^[34] (who only measured either the Ag^+ transfer to AN or to methanol) is unsuitable for generating the sum of the four solvents investigated in our work. By contrast, in our ILSB-network with the excellent m/n ratio of $88/10 = 8.8$ and a consistency standard deviation σ of 0.6 kJ mol^{-1} , the result is more reliable and the consistency is higher. Table 1 displays the agreement of our values with the n-LJP values for measurements without the protic solvent water, where the authors of ref. [34] estimated an uncertainty of about 40 mV or 4 kJ mol^{-1} (the interested reader is referred to p. 7 in the Supporting Information, where this topic is discussed in more detail). It also displays the disagreement with the measurements involving water. This, on the other hand, is consistent with the authors' statement that higher uncertainty is to be expected for those measurements. In addition, all n-LJP values are afflicted with solvent-solvent interactions, Parts C, which is not the case in cell II. Hence, our values for aqueous half-cells are as reliable as all the other values, excluding the identified limitations of the method described above.

Comparison to the TATB assumption

Equation (9) manifests that the conclusion v effectively is an electrochemical TATB assumption with an IL as electrolyte. Indeed, the results of both methods collected in Table 1 are quite similar, indicating the soundness of the underlying idea. Nevertheless, our optimized values differ by up to 2.4 kJ mol^{-11} from the values compiled in an IUPAC-review.^[40] Two reasons might account for this discrepancy. First, the TATB assumption, that is, $\Delta_{\text{r}}G^\circ([\text{TA}]^+) = \Delta_{\text{r}}G^\circ([\text{TB}]^-)$ for all S , is heavily discussed.^[41,50] Experimental^[51] as well as theoretical^[52] indica-

tions suggest that specific interactions of the phenyl rings of the $[\text{TB}]^-$ ion with the water molecules lead to asymmetric hydration of $[\text{TA}]^+$ and $[\text{TB}]^-$. Particularly, $[\text{TA}]^+$ is considered to be less solvated in water than $[\text{TB}]^-$. This, in turn, would mean for cationic Gibbs energy transfer values from water to non-aqueous solvents determined with the TATB method too positive values, that is, the absolute values would be biased. In Table 1 those values indeed are more positive than the values obtained with the ILSB method. We observe that, within $[\text{N}_{2225}]^+$ and $[\text{NTf}_2]^-$, neither phenyl rings – with their $\text{sp}^2 \text{ C-H}$ bonds able to form weak hydrogen bonds – nor any other specific molecular sites are present that would support the formation of short-range directed interactions with solvent molecules leading to asymmetric solvation. Therefore, we expect that all residual interactions between IL ions and solvent are essentially very weak and hence negligible (see also the computed data in Table 2).

Second, and perhaps more relevant is the fact that the tabulated TATB values are effectively combinations of independent investigations obtained with different methods that were subjected to a more or less arbitrary weighting,^[40] that is, most are not pure TATB values. For example, the value for the transfer of Ag^+ from H_2O to AN consists of a weighted mean of eighteen values (four weighted with 1, nine with 0.5, three with 0.2, two with 0.1) obtained with six different methods (inter alia two n-LJP and four ferrocene values). Nine of them are TATB values (with one exception all are even more positive than the tabulated value (!), and their scatter is about 30 kJ mol^{-11} ; Table 1), four weighted with 1, four with 0.5 and one with 0.2. In addition, Marcus adjusted some of the other values by up to 15 kJ mol^{-1} without giving details on the criteria. Hence, the recommended "TATB values" were arbitrarily processed, thereby introducing a distortion between individual values, that is, a relative bias. These two aspects lead us to prefer the results of the method presented here. Nevertheless, our optimized values listed in Table 1 lie within the typically given uncertainty of the TATB method of 6 kJ mol^{-1} .^[53]

Comparison to the ferrocene assumption

Mainly for pragmatic reasons, the IUPAC recommended the use of Fc^+/Fc as a reference redox system in non-aqueous media in 1984,^[54] although it had been known that the results obtained with the ferrocene assumption, that is, $\Delta_{\text{r}}G^\circ(\text{Fc}) = \Delta_{\text{r}}G^\circ(\text{Fc}^+)$ for all S , differ considerably from the TATB and the n-LJP values.^[55] With the ferrocene assumption, the solvent dependent electrostatic terms of the Gibbs solvation energy of the Fc^+ ion are neglected.^[56] This term increases with the permittivity of the solvents.^[26] Moreover, quadrupole-solvent dipole interactions occur in the Fc-molecule.^[57] Measurements of the partial molar entropy difference between Fc and Fc^+ ions in different solvents indicate specific ion-dipole interactions.^[58] In particular, for water the discrepancies are high, possibly because of hydrogen bonds.^[59] Under discussion are also ion pairing and formation of Fc-Fc^+ units.^[60] Eventually, the redox potential of Fc^+/Fc has been confirmed as being solvent-dependent and

related to the solvent's permittivity.^[61] To account for these problems, the Fc^+/Fc values quoted in ref. [41] contain electrostatic contributions as well as effects due to preferable orientation of solvent dipoles towards solutes. This is described with a pre-existing electric field, the so-called "intrapphase potential" ξ . However, the given values rely on some quantum chemical calculations as well as on some estimates, inter alia of the surface potential χ of a phase and of ξ .

Despite all these efforts to improve the method, the differences to the quoted TATB, n-LJP and our values are still high. To our conviction, the Fc^+/Fc values are inferior to our optimized values given in Table 1 that, using assumption v and the above discussion (almost) equal $\Delta_{tr}G(Ag^+, S_1 \rightarrow S_2)$.

Prospects for the method and unifying $E_{abs}^{H_2O}$ redox scale

Any electrochemical half-cell can be included as a node of an extensive network, analysis of which yields a consistent data set, if the individual $S|IL$ boundaries are constant. Therefore, we currently continue this work with additional half-cells containing further solvents but also additional redox systems, particularly anionic ones, to arrive at x_{ii} . If it turns out that the x_{ii} are constant (by experimental evidence) and negligible (by computational or experimental evidence), then the measured data are true Gibbs transfer energies. If it turns out that the x_{ii} are only constant but not negligible, they can be processed if the x_{ii} are known. In any case, that is, even if the x_{ii} remain unknown, a consistent data set of Gibbs transfer energies is obtained, which enables a unified scale to be built.

With the data set obtained in this work, such a unified scale can already be constructed. Any observed potential value of a redox system present in one of the investigated solvents S measured with respect to the system $Ag^+(S)/Ag(s)$ can be implemented into the unified $E_{abs}^{H_2O}$ scale (Table 3) or also the full two-dimensional PPM (Figure 1). In addition, values measured with respect to those systems can be implemented as well and so forth. This eventually leads to a manifold of redoxities (reduction potentials) of redox systems that can be compared between solvents, and – including measurements with the hydrogen electrode – acidities of acid-base systems.

For example, Table 3 includes, among others, the redox system $Fc^+(solv, S)/Fc(solv, S)$ that was measured directly ($S = AN, DMF$) or via the redox system $H^+(solv, S)/H_2(g)$ ($S = PC$) with respect to the redox system $Ag^+(solv, S)/Ag(s)$. This redox system is recommended by the IUPAC as reference system and enables one to connect all values referred to Fc^+/Fc to the unified $E_{abs}^{H_2O}$ scale. For example, the value of $E_{AN}^{o'} = 1.21$ V of the recently presented strong de-electronator "phenazine^F" (the radical cation salt of perfluoro-5,10-bis(perfluorophenyl)-5,10-dihydrophenazine)^[62] was measured in AN with the redox system Fc^+/Fc as reference. Applying the entry Fc^+/Fc ($S = AN$) in Table 3 (+ 0.48 V) on the measured value gives $E_{abs}^{o'/H_2O} = 1.21 + 0.48 = 1.69$ V. Thus, its de-electronation power can easily be identified as being as high as that of the system $Au^+/Au(s)$ in H_2O .^[63]

Table 3. A selection of redox systems including some common reference systems in the realm of unified redoxity linked to the $E_{abs}^{H_2O}(Ag^+(solv, S)/Ag(s))$ values from this work. The physical state of the species is "solvated in the solvent S " (solv, S), if not otherwise stated (g = gaseous, s = solid). Note, that some authors did not specify E^o but $E^{o'}$ or $E_{1/2}$. Cc = cobaltocene = $Co(\eta^5-C_5H_5)_2$.

Redox system	$E_{abs}^{H_2O}/V$	S	Ref.
$Ag^+/Ag(s)$	0.964	PC	this work
$Ag^+/Ag(s)$	0.799	H_2O	[63]
I_2/I^-	0.620	H_2O	[63]
$Ag^+/Ag(s)$	0.579	DMF	this work
I_3^-/I^-	0.540	H_2O	[64]
$Ag^+/Ag(s)$	0.539	AN	this work
Fc^+/Fc	0.483	AN	[65]
Fc^+/Fc	0.445	PC	[66]
Fc^+/Fc	0.431	DMF	[67]
$H^+/H_2(g)$	0.413	AN	[68]
Fc^+/Fc	0.400	H_2O	[69]
$H^+/H_2(g)$	0.369	PC	[70]
I_2/I^-	0.373	AN	[64]
I_2/I^-	0.364	PC	[64]
SCE_{H_2O}	0.241	H_2O	[71]
$AgCl_{H_2O}$	0.197	H_2O	[71]
I_3^-/I^-	0.163	AN	[64]
I_3^-/I^-	0.135	PC	[64]
$Me_{10}Fc^+/Me_{10}Fc$	0.109	H_2O	[72]
$H^+/H_2(g)$	0.000	H_2O	[63]
$Me_{10}Fc^+/Me_{10}Fc$	-0.027	AN	[72]
$Me_{10}Fc^+/Me_{10}Fc$	-0.049	DMF	[72]
$Me_{10}Fc^+/Me_{10}Fc$	-0.050	PC	[72]
$H^+/H_2(g)$	-0.189	DMF	[68]
Cc^+/Cc	-0.85	PC	[73]
Cc^+/Cc	-0.87	AN	[74]
Cc^+/Cc	-0.87	DMF	[73]
Cc^+/Cc	-0.96	H_2O	[74]

In addition, a great many tabulated redox potential data can be integrated into the unified $E_{abs}^{H_2O}$ scale using a similar approach. In the S.I., we exemplarily did work out relations for the photoelectrochemically relevant tris(2,2'-bipyridine)ruthenium(II) ion $[Ru(bipy)_3]^{2+}$ that undergoes seven heterogeneous one-electron transfer reactions, depending on the solvent.

Thus, all redox potential data, self-measured or documented can be tied to the $E_{abs}^{H_2O}$ scale with the values collected in Table 3, and can be unifyingly compared with each other over solvent boundaries. As the values of Table 3 were measured within one solvent, they are free of LJPs. However, some of the used cells were constructed with reference electrode compartments in one way or another, thus it is not entirely excluded that they may contain diffusion potentials (at most a few tens of millivolts). An extended version of Table 3 can be found in the Supporting Information, which contains some more redox systems along with details and comments.

Yet, all values included with Table 3 have to be used with the awareness that, as long as the x_{ii} are not determined experimentally, they are assumed as zero (assumption v), as supported by our quantum chemical computations (Table 2).

Conclusion

We conclude our findings using the notation of Izutsu: for cell II, one has to consider Parts A, B and C of LJPS₁ and LJPS₂ caused by each electrolyte AgZ and [N₂₂₂₅] [NTf₂] (= SB). The results published earlier were:^[32]

I. Parts A_{AgZ} and Parts B_{AgZ} are ineffective (therefore, we use Equation (S4)).

II. Parts A_{SB} cancel.

The results of this work are:

III. Parts B_{SB} most likely cancel out to a large extent, or completely (assumption v).

IV. Parts C are not present.

In terms of Equation (7), the conclusion reads alternatively:

V. The liquid junction potentials $E_{j,1}$ and $E_{j,2}$ are determined exclusively by the IL ions, and are therefore constant in magnitude (although unknown).

VI. Their sum $x_{II} = E_{j,1} + E_{j,2}$ is probably very small, measurable in principle, and can be reasonably assumed to be negligible (assumption v).

Thus, based on these findings, the “ideal” ILSB method is virtually free of LJP contributions, and delivers the currently most accurate experimental Gibbs energies of transfer of a single ion. In contrast to other methods, the consistency is high and was shown by a solid statistical analysis to be 0.6 kJ mol⁻¹ resulting from the compilation of 87 values measured over 10 half-cells between four solvents. Being free from direct solvent-solvent interactions, the “ideal” ILSB provides considerable advantages over other methods, also due to the nontoxicity of the IL used, in contrast to the picrates used by Alexander et al.^[34] Furthermore, with a suitable anionic redox system, the thermodynamically rigorous determination of the LJP's contribution of cell II is possible. Considering the small difference of our results to the quoted TATB values, the x_{II} are small or – accepting the results of the computation with the CPCM model as an approximation – even zero. Thus, we recommend the use of this “ideal” ILSB setup to determine Gibbs energies of transfers of single ions. We note that this IL is commercially available with the company IoLiTec.

Last, not least we have shown that all redox potential data, self-measured or documented and measured in one of our four investigated solvents, can be unified to the $E_{abs}^{H_2O}$ scale with the values collected in Table 1 or 3. They can be compared with each other even over solvent boundaries. Ongoing work will considerably increase the number of solvents available.

Experimental Section

Electrochemical measurements were carried out under argon by using standard Schlenk techniques with self-built half cells and a salt bridge with PEEK capillaries (125 μm diameter) at both ends. This setup was built up in a Faraday cage. E_{II} of all measurements were obtained from open-circuit-potential experiments using the potentiostat VMP3 (Bio-Logic Science Instruments) controlled by a computer through the software EC-Lab (V 11.21, Bio-Logic Science Instruments). Ag wires (MaTeck, 99.99%) were used as working and counter/reference electrodes.

Uncertainty: The measurement error due to inaccuracies in the concentration and dilution errors was calculated to be 5–6 mV. For this, the experimental steps for the preparation of each half cell solution (preparing the stock solution by weighing the silver salt and adding the solvent, dilution to the desired measurement concentration) were analyzed and assigned with an adequate error. For reasons of simplicity the resulted error was obtained by adding the maximum possible error of each experimental step. Errors can only be estimated for (solvation)-concentration cells since no absolute values can be calculated. Therefore, the estimation of the measurement error is based on the change of expected MSA values by variation of the concentration. Together with the inaccuracy of the potentiostat of about 2 mV the overall uncertainty is assumed to be about 7–8 mV in all measurements.

Chemicals: Ag[BF₄] (ChemPur, 99%), Ag[OTf] (Sigma-Aldrich, 99 + %) and Ag[SbF₆] (AlfaAesar, 99%) were used as purchased. Ag[NTf₂] was prepared according to literature^[75] by mixing Ag₂CO₃ and H[NTf₂], which was obtained from Li[NTf₂] (Sigma-Aldrich) and H₂SO₄.^[76] Ag[PF₆] was synthesized by reacting AgF with Li[PF₆].^[77] [N₂₂₂₅][NTf₂] was obtained by mixing Li[NTf₂] and [N₂₂₂₅]Br by a small variation of the procedure from literature namely extracting the IL with dichloromethane. [N₂₂₂₅]Br was synthesized by mixing freshly distilled NEt₃ and 1-Bromopentane (Merck, ≥ 98 %).

NMR spectra were recorded on a BRUKER Avance 200 MHz, a BRUKER Avance III HD 300 MHz or a BRUKER Avance II + 400 MHz WB spectrometer. ¹H NMR chemical shifts are reported in ppm (δ) relative to tetramethylsilane (TMS) and referenced using the chemical shifts of residual protio solvent resonances (CD₂Cl₂: δ = 5.32 ppm, CDCl₃: δ = 7.26 ppm). Data analysis was performed using Bruker TOPSPIN 3.2 software.

The **DOSY NMR spectra** for propylene carbonate and dimethylformamide were recorded on a Bruker AVANCE II + 400 MHz NMR spectrometer with a 5 mm TBO probe head with a z axis gradient coil with a maximum gradient strength of 50 G/cm⁻¹. Measurements were performed at 298 K in 5 mm NMR tubes with J. Young valves using a stimulated echo sequence.

The **DOSY NMR spectra** for D₂O and acetonitrile were recorded on a BRUKER Avance DSX 500 spectrometer equipped with a Diff30 gradient unit and BAFPA-40 amplifier. Measurements were recorded at 297 ± 2 °C using the “diffSte” pulse program. The standard error of the resulting diffusion measurements is estimated to be about 5%, including temperature fluctuations.

The spectra were processed with the TOPSPIN 3.2 and 3.6.1 software. After Fourier transformation and baseline correction, diffusion coefficients were calculated by exponential fits with the T1/T2 module of TOPSPIN.

Acknowledgements

This work was funded through the European Metrology Programme for Innovation and Research (EMPIR) Project 17FUN09 “Realisation of a Unified pH Scale”. The EMPIR is jointly funded by the EMPIR participating countries within the European Association of National Metrology Institutes (EURAMET e.V.) and the European Union. We further acknowledge support of the DFG (KR2046/36-1). The work of IL was additionally supported by the Estonian Research Council grant PRG690. Open Access funding enabled and organized by Projekt DEAL.

Conflict of Interest

The authors declare no conflict of interest.

Data Availability Statement

The data that support the findings of this study are available in the supplementary material of this article.

Keywords: electrochemistry · ionic liquids · salt bridges · single ion Gibbs transfer energy · thermodynamics

- [1] G. Job, F. Herrmann, *Eur. J. Phys.* **2006**, *27*, 353.
- [2] E. A. Guggenheim, *J. Phys. Chem.* **1929**, *33*, 842.
- [3] M. Sastre, J. A. Santaballa, *J. Chem. Educ.* **1989**, *66*, 403.
- [4] R. P. Buck, S. Rondinini, A. K. Covington, F. G. K. Baucke, C. M. A. Brett, M. F. Camoes, M. J. T. Milton, T. Mussini, R. Naumann, K. W. Pratt, et al., *Pure Appl. Chem.* **2002**, *74*, 2169.
- [5] A. L. Rockwood, *ChemPhysChem* **2015**, *16*, 1978.
- [6] A. Ferse, B. Ferse, *Electrochim. Acta* **2016**, *192*, 497.
- [7] R. E. Cohen, T. Cvitas, J. G. Frey, B. Holmström, K. Kuchitsu, R. Marquardt, I. Mills, F. Pavese, M. Quack, J. Stohner, et al., *Quantities, Units and Symbols in Physical Chemistry*, International Union of Pure and Applied Chemistry, RSC Publishing, **2007**.
- [8] D. Himmel, V. Radtke, B. Butschke, I. Krossing, *Angew. Chem. Int. Ed.* **2018**, *57*, 4386; *Angew. Chem.* **2018**, *130*, 4471.
- [9] S. Trasatti, *Electrochim. Acta* **1990**, *35*, 269.
- [10] S. Trasatti, *Pure Appl. Chem.* **1986**, *58*, 955.
- [11] P. Hünenberger, M. Reif, *Single-Ion Solvation. Experimental and Theoretical Approaches to Elusive Thermodynamic Quantities*, The Royal Society of Chemistry, Cambridge, **2011**.
- [12] It is important to be aware that the standard states and measured values can be given with respect to different conventions.^[17] In this work, all values are given in the mol L⁻¹ scale. In addition, the here given value of $\Delta_{\text{sol}}G^{\circ}(\text{H}^+, \text{H}_2\text{O}) = -1105 \pm 8 \text{ kJ mol}^{-1}$ (value 1) is obtained with the cluster pair approximation and is given with respect to the EC-B convention.^[19] Another recommended value is $-1100 \pm 5 \text{ kJ mol}^{-1}$ (value 2) given in the mol kg⁻¹ scale with respect to the EC-FD convention. For the proton, the EC-B value is shifted by about -3.6 kJ mol^{-1} with respect to the EC-FD value (for other ions the shift is negligible). For hydration, the distinction between the mol L⁻¹ and the mol kg⁻¹ scale is considered to be negligible (ca. 0.007 kJ mol⁻¹). The value 2 itself, however, is a mean of 98 values (25 directly published as such, and the authors deduced the other by, for example, real potentials combined with estimates of the surface potential of water) published since 1930. The PPM concept remains unaffected by the conventions, even if the individual values change slightly: pH_{abs} of aqueous solution under standard conditions (relative activity $a(\text{H}^+) = 1$) with value 1 is 193.5 and with value 2 is 192.7. Changing the mol L⁻¹ scale into the mol kg⁻¹ scale, the pH_{abs} value changes by 1 pH unit for the tenfold increase or decrease of the solvents density compared to 1 kg L⁻¹. Most solvents lie in the range of 0.75–1.25 kg L⁻¹, thus the changes lie in the range of about -0.1 to $+0.1$ pH units depending on the solvent.
- [13] V. Radtke, D. Himmel, K. Pütz, S. K. Goll, I. Krossing, *Chem. Eur. J.* **2014**, *20*, 4194.
- [14] S. Trasatti, *J. Electroanal. Chem.* **1982**, *139*, 1.
- [15] E. Kanevskii, *Zh. Fiz. Khim.* **1948**, *22*, 1397.
- [16] D. Himmel, S. K. Goll, I. Leito, I. Krossing, *Angew. Chem. Int. Ed.* **2010**, *49*, 6885; *Angew. Chem.* **2010**, *122*, 7037.
- [17] a) J. E. Bartmess, *J. Phys. Chem.* **1994**, *98*, 6420; b) M. B. Ewing, T. H. Lilley, G. M. Olofsson, M. T. Ratzsch, G. Somsen, *Pure Appl. Chem.* **1994**, *66*, 533; c) V. Radtke, D. Stoica, I. Leito, F. Camões, I. Krossing, B. Anes, M. Roziková, L. Delebeeck, S. Veltzé, T. Näykki, et al., *Pure Appl. Chem.* **2021**, *93*, 1049.
- [18] A. Suu, L. Jalukse, J. Liigand, A. Kruve, D. Himmel, I. Krossing, M. Rosés, I. Leito, *Anal. Chem.* **2015**, *87*, 2623.
- [19] M. D. Tissandier, K. A. Cowen, W. Y. Feng, E. Gundlach, M. H. Cohen, A. D. Earhart, J. V. Coe, T. R. Tuttle, *J. Phys. Chem. A* **1998**, *102*, 7787.
- [20] a) L. P. Santos, T. R. D. Ducati, L. B. S. Balestrin, F. Galembeck, *J. Phys. Chem. C* **2011**, *115*, 11226; b) F. Galembeck, T. A. L. Burgo, *Chemical Electrostatics. New Ideas on Electrostatic Charging: Mechanisms and Consequences*, Springer International Publishing, Cham, s.l., **2017**; c) C. Richmonds, M. Witzke, B. Bartling, S. W. Lee, J. Wainright, C.-C. Liu, R. M. Sankaran, *J. Am. Chem. Soc.* **2011**, *133*, 17582; d) P. J. Bruggeman, R. R. Frontiera, U. R. Kortshagen, M. J. Kushner, S. Linic, G. C. Schatz, H. Andaraarachchi, S. Exarhos, L. O. Jones, C. M. Mueller et al., *J. Appl. Phys.* **2021**, *129*, 200902; e) K.-M. Weitzel, *Curr. Opin. Electrochem.* **2021**, *26*, 100672.
- [21] J. O. Bockris, A. K. Reddy, *Modern Electrochemistry*, Plenum, New York, **1970**.
- [22] A. J. Bard, G. Inzelt, F. Scholz, (Eds.) *Electrochemical Dictionary*, Springer, Berlin, Heidelberg, **2008**.
- [23] L. Onsager, *Phys. Rev.* **1931**, *37*, 405.
- [24] A. J. Staverman, *Trans. Faraday Soc.* **1952**, *48*, 176.
- [25] O. Popovych, R. G. Bates, *Crit. Rev. Anal. Chem.* **1970**, *1*, 73.
- [26] a) A. J. Parker, R. Alexander, *J. Am. Chem. Soc.* **1968**, *90*, 3313; b) Y. Marcus, *Pure Appl. Chem.* **1986**, *58*, 1721.
- [27] J. F. Coetzee, W. K. Istone, *Anal. Chem.* **1980**, *52*, 53.
- [28] K. Izutsu, *Electrochemistry in Nonaqueous Solutions*, Wiley-VCH, Weinheim, **2002**.
- [29] K. Izutsu, *Anal. Sci.* **2011**, *27*, 685.
- [30] V. Radtke, A. Ermantraut, D. Himmel, T. Koslowski, I. Leito, I. Krossing, *Angew. Chem. Int. Ed.* **2018**, *57*, 2344.
- [31] M. Alfenaar, C. L. de Ligny, A. G. Remijnse, *Recl. Trav. Chim. Pays-Bas* **1967**, *86*, 986.
- [32] A. Ermantraut, V. Radtke, N. Gebel, D. Himmel, T. Koslowski, I. Leito, I. Krossing, *Angew. Chem. Int. Ed.* **2018**, *57*, 2348.
- [33] R. G. Bates, *Determination of pH*, Wiley, New York, **1973**.
- [34] R. Alexander, A. J. Parker, J. H. Sharp, W. E. Waghorne, *J. Am. Chem. Soc.* **1972**, *94*, 1148.
- [35] B. G. Cox, A. J. Parker, W. E. Waghorne, *J. Am. Chem. Soc.* **1973**, *95*, 1010.
- [36] L. Blum, *Mol. Phys.* **1975**, *30*, 1529.
- [37] U. P. R. M. Preiss, J. M. Slattery, I. Krossing, *Ind. Eng. Chem. Res.* **2009**, *48*, 2290.
- [38] S. Na, A. Bauß, M. Langenmaier, T. Koslowski, *Phys. Chem. Chem. Phys.* **2017**, *19*, 18938.
- [39] a) S. Tshepelevitsh, A. Kütt, M. Lökov, I. Kaljurand, J. Saame, A. Heering, P. G. Plieger, R. Vianello, I. Leito, *Eur. J. Org. Chem.* **2019**, *2019*, 6735; b) E. Paenurk, K. Kaupmees, D. Himmel, A. Kütt, I. Kaljurand, I. A. Koppel, I. Krossing, I. Leito, *Chem. Sci.* **2017**, *8*, 6964; c) J. Saame, T. Rodima, S. Tshepelevitsh, A. Kütt, I. Kaljurand, T. Haljasorg, I. A. Koppel, I. Leito, *J. Org. Chem.* **2016**, *81*, 7349.
- [40] Y. Marcus, *Pure Appl. Chem.* **1983**, *55*, 977.
- [41] L. I. Krishtalik, *Electrochim. Acta* **2008**, *53*, 3722.
- [42] J. Badoz-Lambling, J. C. Bardin, *Electrochim. Acta* **1974**, *19*, 725.
- [43] Y. Matsubara, D. C. Grills, Y. Koide, *ACS Omega* **2016**, *1*, 1393.
- [44] T. Kakiuchi, N. Tsujioka, S. Kurita, Y. Iwami, *Electrochem. Commun.* **2003**, *5*, 159.
- [45] D. Himmel, S. K. Goll, I. Leito, I. Krossing, *Chemistry A European Journal* **2011**, *17*, 5808.
- [46] V. Barone, M. Cossi, *J. Phys. Chem. A* **1998**, *102*, 1995.
- [47] Frank Neese, *Wiley Interdiscip. Rev.: Comput. Mol. Sci.* **2022**, e1606.
- [48] a) C. Riplinger, B. Sandhoefer, A. Hansen, F. Neese, *J. Chem. Phys.* **2013**, *139*, 134101; b) Y. Guo, C. Riplinger, U. Becker, D. G. Liakos, Y. Minenkov, L. Cavallo, F. Neese, *J. Chem. Phys.* **2018**, *148*, 11101.
- [49] F. Weigend, R. Ahlrichs, *Phys. Chem. Chem. Phys.* **2005**, *7*, 3297.
- [50] a) J. F. Coetzee, W. R. Sharpe, *J. Phys. Chem.* **1971**, *75*, 3141; b) J. I. Kim, *J. Phys. Chem.* **1978**, *82*, 191; c) J. I. Kim, *Z. Phys. Chem.* **1978**, *113*, 129; d) J. I. Kim, *Bull. Soc. Chim. Belg.* **1986**, *95*, 435; e) Y. Shao, A. A. Stewart, H. H. Girault, *J. Chem. Soc. Faraday Trans.* **1991**, *87*, 2593; f) W. R. Fawcett, *J. Phys. Chem.* **1993**, *97*, 9540; g) J. Stangret, E. Kamienska-Piotrowicz, *J. Chem. Soc. Faraday Trans.* **1997**, *93*, 3463; h) T. P. Pollard, T. L. Beck, *J. Chem. Phys.* **2014**, *141*, 18 C512; i) T. P. Pollard, T. L. Beck, *J. Chem. Phys.* **2018**, *148*, 222830; j) M. M. Reif, P. H. Hünenberger, *J. Phys. Chem. B* **2016**, *120*, 8485; k) T. S. Hofer, P. H. Hünenberger, *J. Chem. Phys.* **2018**, *148*, 222814; l) T. T. Duignan, M. D. Baer, C. J. Mundy, *J. Chem. Phys.* **2018**, *148*, 222819.
- [51] R. Scheu, B. M. Rankin, Y. Chen, K. C. Jena, D. Ben-Amotz, S. Roke, *Angew. Chem. Int. Ed.* **2014**, *53*, 9560; *Angew. Chem.* **2014**, *126*, 9714.
- [52] a) R. Schurhammer, G. Wipff, *J. Phys. Chem. A* **2000**, *104*, 11159; b) M. Lesniewski, M. Śmiechowski, *J. Chem. Phys.* **2018**, *149*, 171101.
- [53] Y. Marcus, M. J. Kamlet, R. W. Taft, *J. Phys. Chem.* **1988**, *92*, 3613.
- [54] G. Gritzner, J. Kuta, *Pure Appl. Chem.* **1984**, *56*, 461.

- [55] I. M. Kolthoff, M. K. Chantooni, *J. Phys. Chem.* **1972**, *76*, 2024.
- [56] J. W. Diggle, A. J. Parker, *Electrochim. Acta* **1973**, *18*, 975.
- [57] M. Alfenaar, *J. Phys. Chem.* **1975**, *79*, 2200.
- [58] S. Sahami, M. J. Weaver, *J. Solution Chem.* **1981**, *10*, 199.
- [59] P. A. Lay, *J. Phys. Chem.* **1986**, *90*, 878.
- [60] J. T. Hupp, *Inorg. Chem.* **1990**, *29*, 5010.
- [61] M. R. McDevitt, A. W. Addison, *Inorg. Chim. Acta* **1993**, *204*, 141.
- [62] M. Schorpp, T. Heizmann, M. Schmucker, S. Rein, S. Weber, I. Krossing, *Angew. Chem. Int. Ed.* **2020**, *59*, 9453; *Angew. Chem.* **2020**, *132*, 9540.
- [63] S. G. Bratsch, *J. Phys. Chem. Ref. Data* **1989**, *18*, 1.
- [64] C. L. Bentley, A. M. Bond, A. F. Hollenkamp, P. J. Mahon, J. Zhang, *J. Phys. Chem. C* **2015**, *119*, 22392.
- [65] I. M. Kolthoff, F. G. Thomas, *J. Phys. Chem.* **1965**, *69*, 3049.
- [66] A. K. Srivastava, L. M. Mukherjee, *J. Electroanal. Chem. Interfacial Electrochem.* **1984**, *160*, 209.
- [67] A. V. Benedetti, *Eclat. Quim. J.* **1984**, *9*, 13.
- [68] V. Fourmond, P.-A. Jacques, M. Fontecave, V. Artero, *Inorg. Chem.* **2010**, *49*, 10338.
- [69] A. M. Bond, E. A. McLennan, R. S. Stojanovic, F. G. Thomas, *Anal. Chem.* **1987**, *59*, 2853.
- [70] L. M. Mukherjee, R. G. Bates, *J. Electroanal. Chem. Interfacial Electrochem.* **1985**, *187*, 73.
- [71] A. J. Bard, L. R. Faulkner, *Electrochemical Methods. Fundamentals and Applications*, 2nd ed., Wiley, New York, **2001**.
- [72] I. Noviandri, K. N. Brown, D. S. Fleming, P. T. Gulyas, P. A. Lay, A. F. Masters, L. Phillips, *J. Phys. Chem. B* **1999**, *103*, 6713.
- [73] T. Kakutani, Y. Morihoro, M. Senda, R. Takahashi, K. Matsumoto, *Bull. Chem. Soc. Jpn.* **1978**, *51*, 2847.
- [74] R. S. Stojanovic, A. M. Bond, *Anal. Chem.* **1993**, *65*, 56.
- [75] A. Vij, Y. Y. Zheng, R. L. Kirchmeier, J. M. Shreeve, *Inorg. Chem.* **1994**, *33*, 3281.
- [76] A. C. D. A. Rosa, C. M. Correa, R. Faez, M. A. Bizeto, F. F. Camilo, *RSC Adv.* **2013**, *3*, 26142.
- [77] I. Krossing, A. Reisinger, *Coord. Chem. Rev.* **2006**, *250*, 2721.

Manuscript received: February 16, 2022

Accepted manuscript online: April 21, 2022

Version of record online: May 31, 2022